PHYSICAL REVIEW D **74,** 011501(R) (2006)

Universality and m_X cut effects in $B \to X_s \ell^+ \ell^-$

Keith S. M. Lee,[1] Zoltan Ligeti,[2,1] Iain W. Stewart,[1] and Frank J. Tackmann[2]

[1]*Center for Theoretical Physics, Massachusetts Institute of Technology, Cambridge, Massachusetts 02139, USA*

[2]*Ernest Orlando Lawrence Berkeley National Laboratory, University of California, Berkeley, California 94720, USA*

(Received 20 December 2005; published 14 July 2006)

The most precise comparison between theory and experiment for the $B \to X_s \ell^+ \ell^-$ rate is in the low q^2 region, but the hadronic uncertainties associated with an experimentally required cut on m_X potentially spoil the search for new physics in these decays. We show that a 10%–30% reduction of $\mathrm{d}\Gamma(B \to X_s \ell^+ \ell^-)/\mathrm{d}q^2$ due to the m_X cut can be accurately computed using the $B \to X_s \gamma$ shape function. The effect is universal for all short distance contributions in the limit $m_X^2 \ll m_B^2$, and this universality is spoiled neither by realistic values of the m_X cut nor by α_s corrections. Both the differential decay rate and forward-backward asymmetry with an m_X cut are computed.

DOI: 10.1103/PhysRevD.74.011501 PACS numbers: 13.20.He, 12.38.Bx

I. INTRODUCTION

In the standard model (SM) the flavor-changing neutral current process $B \to X_s \ell^+ \ell^-$ does not occur at tree level and is thus a sensitive probe of new physics. Predicting its rate involves integrating out the W, Z, and t at a scale of order m_W by matching on to the Hamiltonian [1,2]

$$H_W = -\frac{G_F}{\sqrt{2}} V_{tb} V_{ts}^* \Big[\sum_{i=1}^{6} C_i O_i + \frac{1}{4\pi^2} \sum_{i=7}^{10} C_i O_i \Big], \qquad (1)$$

evolving to $\mu = m_b$, and computing matrix elements of H_W. Here $O_1 - O_6$ are four-quark operators and

$$\begin{aligned} O_7 &= \overline{m}_b \bar{s} \sigma_{\mu\nu} e F^{\mu\nu} P_R b, \\ O_8 &= \overline{m}_b \bar{s} \sigma_{\mu\nu} g G^{\mu\nu} P_R b, \\ O_9 &= e^2 (\bar{s} \gamma_\mu P_L b)(\bar{\ell} \gamma^\mu \ell), \\ O_{10} &= e^2 (\bar{s} \gamma_\mu P_L b)(\bar{\ell} \gamma^\mu \gamma_5 \ell), \end{aligned} \qquad (2)$$

where $P_{L,R} = (1 \mp \gamma_5)/2$. Measurements of $C_{7,8,9,10}$ probe flavor-changing neutral currents and test the SM. This can be done with the dilepton invariant mass spectrum, $d\Gamma/dq^2$, with $q^2 = (p_{\ell^+} + p_{\ell^-})^2$. It is calculable in an operator product expansion (OPE), and the nonperturbative corrections are $\mathcal{O}(\Lambda_{\mathrm{QCD}}^2/m_b^2)$ [3,4]. The matching and anomalous dimensions for C_i are known at next-to-next-to-leading log (NNLL) order, as are the perturbative QCD corrections to the matrix elements of O_i [5–7] (except small O_{3-6} terms).

A complication in $B \to X_s \ell^+ \ell^-$ compared with $B \to X_s \gamma$ is that the long distance contributions, $B \to J/\psi X_s$ and $\psi' X_s$ followed by $J/\psi, \psi' \to \ell^+ \ell^-$, are 2 orders of magnitude above the short distance prediction, a fact which is not well understood. Therefore, either theory and data are both interpolated, or the short distance calculation is compared with the data for $q^2 < m_{J/\psi}^2$ or $q^2 > m_{\psi'}^2$. The low q^2 region, $q^2 < 6\ \mathrm{GeV}^2$, allows the most precise comparison with the SM, but requires a cut on the invariant mass of the hadronic final state, $m_X < m_X^{\mathrm{cut}}$. In the latest Belle analysis $m_X^{\mathrm{cut}} = 2\ \mathrm{GeV}$ [8], while *BABAR* uses $m_X^{\mathrm{cut}} = 1.8\ \mathrm{GeV}$ [9]. This cut is to remove backgrounds and will likely be required for quite some time [10]. So far, its effect has been studied only in the Fermi-motion model [11]. [The high q^2 region is unaffected by the m_X cut, but the rate is lower, and calculating it involves an expansion in $\Lambda_{\mathrm{QCD}}/(m_b - \sqrt{q^2})$.]

In this letter we compute the $B \to X_s \ell^+ \ell^-$ rate with an m_X cut in the low q^2 region in a model-independent framework. For $(m_X^{\mathrm{cut}})^2 = \mathcal{O}(\Lambda_{\mathrm{QCD}} m_b)$, the local OPE used in all earlier analyses breaks down and must be replaced by an OPE involving b quark distribution functions (shape functions), as explained below. We will compute

$$\Gamma_{ij}^{\mathrm{cut}} = \int_{q_1^2}^{q_2^2} \mathrm{d}q^2 \int_0^{m_X^{\mathrm{cut}}} \mathrm{d}m_X\, \mathrm{Re}(c_i c_j^*) \frac{\mathrm{d}^2 \Gamma_{ij}}{\mathrm{d}q^2 \mathrm{d}m_X}, \qquad (3)$$

and study the ratios

$$\eta_{ij}(m_X^{\mathrm{cut}}, q_1^2, q_2^2) = \frac{\Gamma_{ij}^{\mathrm{cut}}}{\Gamma_{ij}^0}. \qquad (4)$$

For convenience we define normalization factors

$$\begin{aligned} \Gamma_{ij}^0 &= \frac{\Gamma_0}{m_B^5} \int_{q_1^2}^{q_2^2} \mathrm{d}q^2 \mathrm{Re}(c_i c_j^*) \frac{(m_b^2 - q^2)^2}{m_b^3} G_{ij}, \\ \Gamma_0 &= \frac{G_F^2 m_B^5}{192\pi^3} \frac{\alpha_{\mathrm{em}}^2}{4\pi^2} |V_{tb} V_{ts}^*|^2, \end{aligned} \qquad (5)$$

with kinematic dependence $G_{99} = G_{00} = (2q^2 + m_b^2)$, $G_{77} = 4m_B^2(1 + 2m_b^2/q^2)$, and $G_{79} = 12 m_B m_b$. Here and below, m_b is a short distance mass, such as m_b^{1S} [12]. In Eqs. (3)–(5), $ij = \{77, 99, 00, 79\}$ label contributions of time-ordered products of operators, $T\{O_j^\dagger, O_i\}$. The total decay rate with cuts is the sum of these contributions,

$$\Gamma^{\mathrm{cut}} = \Gamma \Big|_{\substack{m_X < m_X^{\mathrm{cut}} \\ q_1^2 < q^2 < q_2^2}} = \sum_{ij} \Gamma_{ij}^{\mathrm{cut}}. \qquad (6)$$

We will also study $\eta'_{ij} = \eta'_{ij}(p_X^{+\mathrm{cut}}, q_1^2, q_2^2)$, which differs from η_{ij} by the replacement of m_X by $p_X^+ = E_X - |\vec{p}_X|$:

$$\eta'_{ij} = \frac{1}{\Gamma^0_{ij}} \int_{q_1^2}^{q_2^2} \mathrm{d}q^2 \int_0^{p_X^{+\mathrm{cut}}} \mathrm{d}p_X^+ \mathrm{Re}(c_i c_j^*) \frac{\mathrm{d}^2\Gamma_{ij}}{\mathrm{d}q^2 \mathrm{d}p_X^+}. \quad (7)$$

In Eqs. (3)–(7) the short distance coefficients $c_{7,9,0}$ track the $C_{7,9,10}$ dependence in Eq. (1) that one would like to measure. Here $c_7 = C_7^{\mathrm{mix}}(q^2)$, $c_9 = C_9^{\mathrm{mix}}(q^2)$, and $c_0 = C_{10}$ can be obtained from local OPE calculations [13] at each order, as discussed in Ref. [14].

The η_{ij}'s contain the effects of the m_X cut, and are defined with a normalization that makes them less sensitive to the choice of ij. At leading order in $\Lambda_{\mathrm{QCD}}/m_b$ and α_s, η_{ij} give the fraction of events with $m_X < m_X^{\mathrm{cut}}$, and $\eta_{ij} = 1$ for $m_X^{\mathrm{cut}} = m_B$. This interpretation is altered at subleading order by α_s corrections, but knowing η_{ij} at a given order in perturbation theory is still sufficient to determine $\Gamma_{ij}^{\mathrm{cut}}$ and thus the total rate with cuts in Eq. (6), at this order. In principle, η_{ij} depend in a nontrivial way on ij (and q_1^2 and q_2^2) due to different dependence on kinematic variables, α_s corrections, etc. At leading order in $\Lambda_{\mathrm{QCD}}/m_b$, we demonstrate that η_{ij} are actually independent of the choice of ij, a property which we call "universality". We first show this formally in Sec. II at leading order in $p_X^+/m_B \ll 1$ for $\eta'(p_X^{+\mathrm{cut}})$. Then in Sec. III we demonstrate it numerically for the experimentally relevant $\eta(m_X^{\mathrm{cut}})$, including the α_s corrections and phase space effects.

We also compute the decay rate for current experimental cuts. We find that the rate is sensitive to the choice of the cut, and that the cut causes a reduction in the rate by 10%–30%. Since the same shape function occurs in $B \to X_s \ell^+ \ell^-$, $X_u \ell \bar{\nu}$, and $X_s \gamma$, the m_X^{cut} or $p_X^{+\mathrm{cut}}$ dependence in one can be accurately determined from the others, and the magnitude of the reduction can be computed quite accurately. Alternatively, instead of using the theoretical computation of the m_X^{cut} dependence, universality can be exploited to remove the main uncertainties, by normalizing the $B \to X_s \ell^+ \ell^-$ rate to $B \to X_u \ell \bar{\nu}$.

II. m_X CUT EFFECTS AT LEADING ORDER

For simplicity, consider the kinematics in the B meson's rest frame. Since $q = p_B - p_X$,

$$2m_B E_X = m_B^2 + m_X^2 - q^2. \quad (8)$$

If $m_X^2 \ll m_B^2$ and q^2 is not near m_B^2, then $E_X = \mathcal{O}(m_B)$. Since $E_X^2 \gg m_X^2$, p_X is near the light-cone, with $p_X^+ = E_X - |\vec{p}_X| = \mathcal{O}(\Lambda_{\mathrm{QCD}})$ and $p_X^- = E_X + |\vec{p}_X| = \mathcal{O}(m_B)$. Of the variables symmetric in p_{ℓ^+} and p_{ℓ^-} ($p_X^\pm$, E_X, q^2, m_X^2), only two are independent, and we work with q^2 and p_X^+ or m_X. The phase space cuts are shown in Fig. 1.

For the $p_X^+ \ll p_X^-$ region, factorization of the form $\mathrm{d}\Gamma = HJ \otimes \hat{f}^{(0)}$ has been proven for semileptonic and radiative B decays [15], where H contains perturbative physics at $\mu_b \sim m_b$, J at $\mu_i \sim \sqrt{\Lambda_{\mathrm{QCD}} m_b}$, and $\hat{f}^{(0)}(\omega)$ is a universal nonperturbative shape function [16]. This factorization

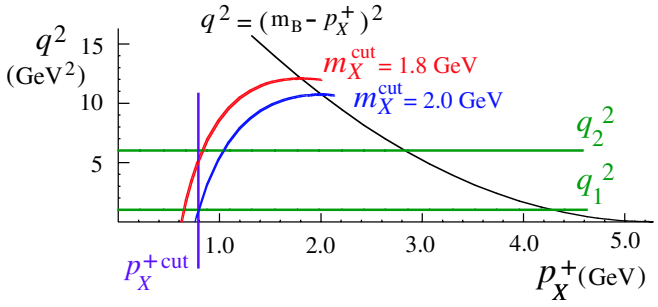

FIG. 1 (color online). Phase space cuts. A substantial part of the rate for $q_1^2 < q^2 < q_2^2$ falls in the rectangle bounded by $p_X^+ < p_X^{+\mathrm{cut}}$.

also applies for $B \to X_s \ell^+ \ell^-$ with the same $\hat{f}^{(0)}$, as long as q^2 is not parametrically small [14].

In the $q^2 < 6$ GeV^2 region, $|C_9^{\mathrm{mix}}(q^2, \mu_0 = 4.8\,\mathrm{GeV})| = 4.52$ to better than 1%, and can be taken to be constant. We neglect α_s corrections in this section and find

$$\begin{aligned}\frac{\mathrm{d}\Gamma}{\mathrm{d}p_X^+ \mathrm{d}q^2} = \hat{f}^{(0)}(p_X^+) \frac{\Gamma_0}{m_B^5} \frac{[(m_B - p_X^+)^2 - q^2]^2}{(m_B - p_X^+)^3} \\ \times \Big\{ (|C_9^{\mathrm{mix}}|^2 + C_{10}^2)[2q^2 + (m_B - p_X^+)^2] \\ + 4m_B^2 |C_7^{\mathrm{mix}}|^2 \Big[1 + \frac{2(m_B - p_X^+)^2}{q^2} \Big] \\ + 12 m_B \,\mathrm{Re}[C_7^{\mathrm{mix}} C_9^{\mathrm{mix}*}](m_B - p_X^+) \Big\}, \end{aligned} \quad (9)$$

where $\hat{f}^{(0)}(\omega)$ has support in $\omega \in [0, \infty)$. As a function of p_X^+, the kinematic terms in Eq. (9) vary *only* on a scale m_B, while $\hat{f}^{(0)}(p_X^+)$ varies on a scale Λ_{QCD}. Writing $m_B = m_b + \bar{\Lambda}$ and expanding in $(p_X^+ - \bar{\Lambda})/m_B$ decouple the p_X^+ and q^2 dependences in Eq. (9), and give exactly the local OPE prefactors, $(m_b^2 - q^2)^2 G_{ij}(q^2)$, used in Eq. (5). For $\eta'_{ij}(p_X^{+\mathrm{cut}}, q_1^2, q_2^2)$, the p_X^+ integration is over a rectangle in Fig. 1, whose boundaries do not couple p_X^+ and q^2. Thus, with the above expansion, we find $\eta'_{ij} = \eta'$, where

$$\eta' = \int \mathrm{d}p_X^+ \hat{f}^{(0)}(p_X^+), \quad (10)$$

independent of ij and q_1^2, q_2^2. While the m_X cut retains more events than the p_X^+ cut, the latter may give theoretically cleaner constraints on short distance physics when statistical errors become small.

The effect of the m_X cut is q^2 dependent, because the upper limit of the p_X^+ integration is q^2 dependent, as shown in Fig. 1. When we include the full p_X^+ dependence in Eq. (9), the universality of $\eta_{ij}(m_X^{\mathrm{cut}}, q_1^2, q_2^2)$ is maintained to better than 3% for 1 GeV$^2 \le q_1^2 \le 2$ GeV^2, 5 GeV$^2 \le q_2^2 \le 7$ GeV^2, and $m_X^{\mathrm{cut}} \ge 1.7$ GeV, because the region where the p_X^+ and q^2 integration limits are coupled has a small effect on the ij dependence. This is exhibited in Fig. 2, where the solid curves show

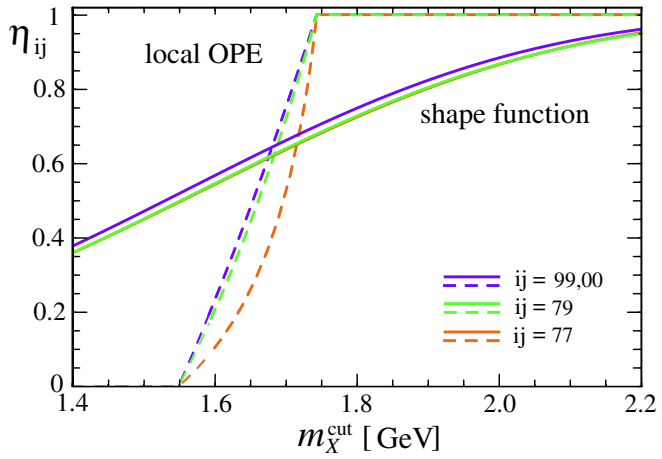

FIG. 2 (color online). $\eta_{ij}(m_X^{\rm cut}, 1\ {\rm GeV}^2, 6\ {\rm GeV}^2)$ as functions of $m_X^{\rm cut}$. The dashed curves show the local OPE result, the solid curves include the leading shape function effects. The uppermost, middle, and lowest curves are $\eta_{00,99}$, η_{79}, and η_{77}, respectively.

$\eta_{ij}(m_X^{\rm cut}, 1\ {\rm GeV}^2, 6\ {\rm GeV}^2)$ with the shape function set to model 1 of [17], with $m_b^{1S} = 4.68$ GeV and λ_1 from [18]. (Taking $q_1^2 = 1\ {\rm GeV}^2$ instead of $4m_\ell^2$ increases the sensitivity to $C_{9,10}$, but one may be concerned by local duality/resonances near $q^2 = 1\ {\rm GeV}^2$. To estimate this uncertainty, assume the ϕ is just below the cut and $\mathcal{B}(B \to X_s\phi) \approx 10 \times \mathcal{B}(B \to K^{(*)}\phi)$. Then $B \to X_s\phi \to X_s\ell^+\ell^-$ is $\sim$2% of the $X_s\ell^+\ell^-$ rate.)

The local OPE results for $\eta_{ij}(m_X^{\rm cut}, q_1^2, q_2^2)$ are obtained by replacing $\hat f^{(0)}(p_X^+)$ by $\delta(\bar\Lambda - p_X^+)$ in Eq. (9). Performing the p_X^+ integral sets $(m_B - p_X^+) = m_b$ and implies $m_X^2 > \bar\Lambda(m_B - q^2/m_b)$. This makes the lower limit on q^2 equal $\max\{q_1^2, m_b[m_B - (m_X^{\rm cut})^2/\bar\Lambda]\}$, and so the η_{ij}'s depend on the shape of $d\Gamma_{ij}$. In Fig. 2 the local OPE results are shown by dashed lines, and clearly $\eta_{77} \neq \eta_{99}$. However, the local OPE is not applicable for $p_X^+ \sim \Lambda_{\rm QCD}$.

The universality of η_{ij} found here could be broken by α_s corrections in the H or J functions, or by renormalization group evolution, since these effects couple p_X^+ and q^2 and have been neglected so far. We consider these next.

III. CALCULATION AND RESULTS AT $\mathcal{O}(\alpha_s)$

A complication in calculating $B \to X_s\ell^+\ell^-$ compared with $B \to X_u\ell\bar\nu$ is that, in the evolution of the effective Hamiltonian down to m_b, $C_9(\mu)$ receives a $\ln(m_W^2/m_b^2)$ enhanced contribution from the mixing of O_2. Thus, formally, $C_9 \sim \mathcal{O}(1/\alpha_s)$, and conventionally one expands the amplitude in α_s, treating $\alpha_s \ln(m_W^2/m_b^2) = \mathcal{O}(1)$ [13]. In the local OPE this is reasonable, since the nonperturbative corrections are small, and at next-to-leading log (NLL) all dominant terms in the rate are included. However, in the shape function region nonperturbative effects are $\mathcal{O}(1)$ and only the rate is calculable, not the amplitude. With the traditional counting, the C_9^2 contribution to the rate would be needed to $\mathcal{O}(\alpha_s^2)$ before the C_{10}^2 terms could be included.

This would be a bad way to organize the perturbative corrections (numerically $|C_9(m_b)| \approx |C_{10}|$). It can be circumvented by using a "split matching" procedure to decouple the perturbation series above and below the scale m_b [14]. This allows us to consider the short distance coefficients $C_7^{\rm mix}$, $C_9^{\rm mix}$, and C_{10} as $\mathcal{O}(1)$ numbers when organizing the perturbation theory at m_b^2 and $m_b\Lambda_{\rm QCD}$.

The rate and the forward-backward asymmetry are

$$\begin{aligned}\frac{d^2\Gamma}{dq^2 dp_X^+} &= \frac{\Gamma_0}{m_B^2} H(q^2, p_X^+) F^{(0)}(p_X^+, p^-),\\ \frac{d^2A_{\rm FB}}{dq^2 dp_X^+} &= \frac{\Gamma_0}{m_B^2} K(q^2, p_X^+) F^{(0)}(p_X^+, p^-),\end{aligned} \tag{11}$$

where $p^- = m_b - q^2/(m_B - p_X^+)$. The hard functions H and K were computed in [14] using soft-collinear effective theory (SCET) [19,20] and split matching. This factorizes the dependence on scales above and below m_b as $\Gamma_{ij} \sim H_1(\mu_0)H_2(\mu_b)F^{(0)}(\mu_b)$, with separate μ_0 and μ_b independence. Up to the order one is working at, H_1 is μ_0 independent, the μ_b dependence in H_2 and $F^{(0)}$ cancels, and $F^{(0)}$ is μ_i independent. The shape function model is specified at μ_Λ. The convolution of jet and shape functions at NLL including α_s corrections is

$$\begin{aligned}F^{(0)}(p_X^+, p^-) &= U_H(p^-, \mu_i, \mu_b)\Bigg(\hat f^{(0)}(p_X^+, \mu_i) + \frac{\alpha_s(\mu_i)C_F}{4\pi}\Bigg\{\Bigg[2\ln^2\frac{p_X^+ p^-}{\mu_i^2} - 3\ln\frac{p_X^+ p^-}{\mu_i^2} + 7 - \pi^2\Bigg]\hat f^{(0)}(p_X^+, \mu_i)\\ &\quad + \int_0^1 \frac{dz}{z}\Bigg[4\ln\frac{z p_X^+ p^-}{\mu_i^2} - 3\Bigg]\Big[\hat f^{(0)}(p_X^+(1-z), \mu_i) - \hat f^{(0)}(p_X^+, \mu_i)\Big]\Bigg\}\Bigg),\\ \hat f^{(0)}(\omega, \mu_i) &= \frac{e^{V_S(\mu_i,\mu_\Lambda)}}{\Gamma(1+\eta)}\Big(\frac{\omega}{\mu_\Lambda}\Big)^\eta \int_0^1 dt\ \hat f^{(0)}[\omega(1-t^{1/\eta}), \mu_\Lambda],\end{aligned} \tag{12}$$

where $\eta = (16/25)\ln[\alpha_s(\mu_\Lambda)/\alpha_s(\mu_i)]$, U_H was computed in Ref. [19], the one-loop jet function in Ref. [21,22], and the shape function evolution up to μ_i in Refs. [19,22] (for earlier calculations, see Refs. [15,23]). The hard coefficients H and K for $B \to X_s\ell^+\ell^-$ are

$$H(q^2, p_X^+) = \frac{[(1-\hat{p}_X^+)^2 - \hat{q}^2]^2}{(1-\hat{p}_X^+)^3}\Big\{[|C_9^{\rm mix}(s,\mu_0)|^2 + C_{10}^2][2\hat{q}^2\Omega_A^2(s,\mu_b) + (1-\hat{p}_X^+)^2\Omega_B^2(s,\hat{p}_X^+,\mu_b)]$$
$$+ 4|C_7^{\rm mix}(\mu_0)|^2\Big[\Omega_C^2(s,\mu_b) + \frac{2(1-\hat{p}_X^+)^2}{\hat{q}^2}\Omega_D^2(s,\mu_b)\Big] + 12\,{\rm Re}[C_7^{\rm mix}(\mu_0)C_9^{\rm mix}(s,\mu_0)^*](1-\hat{p}_X^+)\Omega_E(s,\mu_b)\Big\},$$
$$K(q^2, p_X^+) = -\frac{3\hat{q}^2[(1-\hat{p}_X^+)-\hat{q}^2]^2}{(1-\hat{p}_X^+)^3}\Omega_A(s,\mu_b)\,{\rm Re}\Big\{C_{10}^*\Big[C_9^{\rm mix}(s,\mu_0)\Omega_A(s,\mu_b) + \frac{2(1-\hat{p}_X^+)}{\hat{q}^2}C_7^{\rm mix}(\mu_0)\Omega_D(s,\mu_b)\Big]\Big\}, \quad (13)$$

where $s = q^2/m_b^2$, $\hat{q}^2 = q^2/m_B^2$, $\hat{p}_X^+ = p_X^+/m_B$, and

$$\Omega_A = 1 + \frac{\alpha_s}{\pi}\omega_a^V(s,\mu_b), \qquad \Omega_B = 1 + \frac{\alpha_s}{\pi}\Big[\omega_a^V(s,\mu_b) + \frac{(1-\hat{p}_X^+)^2-\hat{q}^2}{2(1-\hat{p}_X^+)^2}\omega_b^V(s) + \omega_c^V(s)\Big],$$
$$\Omega_C = 1 + \frac{\alpha_s}{\pi}\omega_a^T(s,\mu_b), \qquad \Omega_D = 1 + \frac{\alpha_s}{\pi}[\omega_a^T(s,\mu_b) - \omega_c^T(s)], \qquad \Omega_E = (2\Omega_A\Omega_D + \Omega_B\Omega_C)/3. \quad (14)$$

Here $\alpha_s = \alpha_s(\mu_b)$ and $\omega_i^{V,T}$ are defined in Ref. [14].

For each shape function model, the deviations of the η_{ij}'s from being universal, with all NLL corrections, are still below 3%. Thus, the picture of universality in Fig. 2 remains valid at NLL order. For this reason we can explore the overall shift by just studying η_{00}.

In Fig. 3 we plot $\eta_{00}(m_X^{\rm cut}, 1\ {\rm GeV}^2, 6\ {\rm GeV}^2)$, including the α_s corrections. We use ten different models for $\hat{f}^{(0)}$. Our base model has five parameters, three of which are chosen to obey the known constraints on its moments [22], converted to the $1S$ mass scheme used here. For each of five different choices of the remaining two parameters, we choose two values of the scale, μ_Λ, where the model is specified. The choice of these ten models is guided by making them consistent with the $B \to X_s\gamma$ data. The ten orange, green and purple (medium, light, dark) curves correspond to $m_b^{1S} = 4.68$ GeV, 4.63 GeV, and 4.73 GeV, respectively, with the central values $\mu_0 = \mu_b = 4.8$ GeV and $\mu_i = 2.5$ GeV. The curves with slightly lower [higher] values of η_{00} at large $m_X^{\rm cut}$ correspond to $\mu_\Lambda = 1.5$ GeV [2 GeV]. The spread in the curves gives our determination of the uncertainty from the choice of shape function model and from m_b. For $m_X^{\rm cut} = 2$ GeV, varying μ_b in the range $3.5\ {\rm GeV} < \mu_b < 7.5\ {\rm GeV}$ changes η_{00} by $\pm 6\%$. We find a $\pm 5\%$ variation for $2\ {\rm GeV} < \mu_i < 3\ {\rm GeV}$.

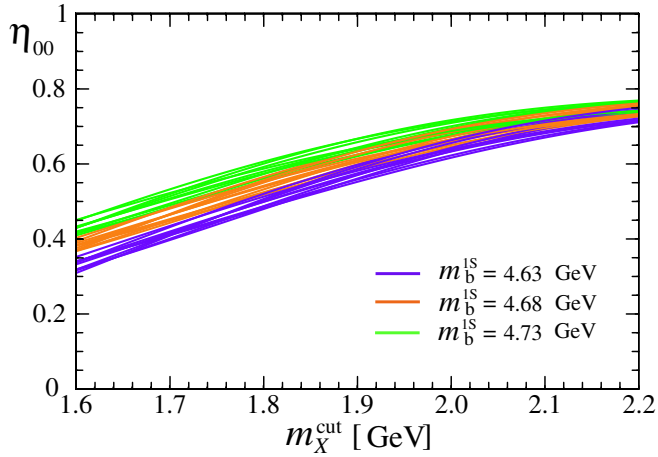

FIG. 3 (color online). $\eta_{00}(m_X^{\rm cut}, 1\ {\rm GeV}^2, 6\ {\rm GeV}^2)$ as a function of $m_X^{\rm cut}$. The orange, green and purple (medium, light, dark) curves show $m_b^{1S} = 4.68$ GeV, 4.63 GeV, and 4.73 GeV, respectively.

Using the c_i's at NLL, for $1\ {\rm GeV}^2 < q^2 < 6\ {\rm GeV}^2$ we obtain cut branching ratios

$$\Gamma^{\rm cut}\tau_B = \begin{cases} (1.20 \pm 0.15) \times 10^{-6} & [m_X^{\rm cut} = 1.8\ {\rm GeV}], \\ (1.48 \pm 0.14) \times 10^{-6} & [m_X^{\rm cut} = 2.0\ {\rm GeV}], \end{cases} \quad (15)$$

where uncertainties are included from m_b, μ_b, μ_i, and $\hat{f}^{(0)}$. Changing μ_0 to 3.5 GeV (10 GeV) changes both of these rates by -2% ($+7\%$), and this uncertainty will be reduced by including NNLL corrections [5–7].

The largest source of universality breaking in the η_{ij}'s and one of the largest uncertainties in the cut rate is due to subleading shape functions, which affect the rate by $\sim 5\%$ for $m_X^{\rm cut} = 2$ GeV and by $\sim 10\%$ for $m_X^{\rm cut} = 1.8$ GeV [24].

If the $m_X^{\rm cut}$ dependence were not universal, it would modify the zero of the forward-backward asymmetry, $A_{\rm FB}(q_0^2) = 0$. For $m_X^{\rm cut} = 2$ GeV we find at NLL $\Delta q_0^2 \approx -0.04{\rm GeV}^2$, much below the higher order uncertainties [6,7]. However, we obtain $q_0^2 = 2.8\ {\rm GeV}^2$, lower than earlier results [6]. The reason is that in the SCET calculation of $A_{\rm FB}$, using K in Eq. (13), the pole mass $m_b^{\rm pole}$ never occurs, only $m_B - p_X^+$ and $\overline{m}_b$ (at this order, $C_7^{\rm mix} = (\overline{m}_b/m_B)C_7^{\rm eff}$ [14]). Thus, schematically, $q_0^2 \sim 2m_b[\overline{m}_b(\mu_0)C_7^{\rm eff}(\mu_0)]/{\rm Re}[C_9^{\rm eff}(q_0^2)]$, and there is no reason to expand $\overline{m}_b$ in terms of $m_b^{\rm pole}$.

In the above analysis, the nonperturbative shape function $f^{(0)}$ was extracted from moments and the $B \to X_s\gamma$ energy spectrum, and this was used as input in determining our $B \to X_s\ell^+\ell^-$ results. The overall 10% theoretical uncertainty in this approach could be reduced by raising the $m_X^{\rm cut}$. An alternative approach would be to keep $m_X^{\rm cut} < m_D$ and measure

$$R = \frac{\Gamma^{\rm cut}(B \to X_s \ell^+ \ell^-)}{\Gamma^{\rm cut}(B \to X_u \ell \bar{\nu})}, \tag{16}$$

with the same cuts used in the numerator and denominator. The dependence of the semileptonic rate on $m_X^{\rm cut}$ is identical to that of $\Gamma_{00}^{\rm cut}$. A measurement of R bypasses the need for a shape function model, because we found that the m_X-cut effects are universal to a very good approximation and therefore cancel between the numerator and denominator of R.

In conclusion, we pointed out that the observed $B \to X_s \ell^+ \ell^-$ rate in the low q^2 region is sensitive to the experimental upper cut on m_X. The reduction in the rate due to this cut is determined by the universal B shape function. In the region of the experimental measurements an OPE exists only for the decay rate and not for the amplitude, a fact that necessitates a reorganization of the usual perturbation expansion. Since one can use the shape function measured in other processes, the sensitivity to new physics is not reduced. We found that the η's for the different operators' contributions are universal to a good approximation. These results also apply for $B \to X_d \ell^+ \ell^-$, which may be studied at a higher luminosity B factory. Subleading $\Lambda_{\rm QCD}/m_b$ as well as NNLL corrections to the rate and the forward-backward asymmetry will be studied in a separate publication [24].

ACKNOWLEDGMENTS

We thank Bjorn Lange for helpful discussions. This work was supported in part by the Director, Office of Science, and Offices of High Energy and Nuclear Physics of the U.S. Department of Energy under the Contract Nos. DE-AC02-05CH11231 (Z. L. and F. T.), and the cooperative research agreement DOE-FC02-94ER40818 (K. L. and I. S.). I. S. was also supported in part by the DOE OJI program and by the Sloan Foundation.

[1] B. Grinstein *et al.*, Nucl. Phys. **B319**, 271 (1989).
[2] G. Buchalla, A. J. Buras, and M. E. Lautenbacher, Rev. Mod. Phys. **68**, 1125 (1996).
[3] A. F. Falk, M. E. Luke, and M. J. Savage, Phys. Rev. D **49**, 3367 (1994).
[4] A. Ali *et al.*, Phys. Rev. D **55**, 4105 (1997).
[5] C. Bobeth, M. Misiak, and J. Urban, Nucl. Phys. **B574**, 291 (2000); H. H. Asatryan *et al.*, Phys. Rev. D **65**, 074004 (2002); C. Bobeth *et al.*, J. High Energy Phys. 4 (2004) 071.
[6] A. Ghinculov *et al.*, Nucl. Phys. **B648**, 254 (2003); H. M. Asatrian *et al.*, Phys. Rev. D **66**, 094013 (2002).
[7] A. Ghinculov *et al.*, Nucl. Phys. **B685**, 351 (2004).
[8] M. Iwasaki *et al.* (Belle Collaboration), Phys. Rev. D **72**, 092005 (2005).
[9] B. Aubert *et al.* (*BABAR* Collaboration), Phys. Rev. Lett. **93**, 081802 (2004).
[10] J. Berryhill, SLAC-INT Workshop, Seattle, http://www.int.washington.edu/talks/WorkShops/int_05_1/.
[11] A. Ali and G. Hiller, Phys. Rev. D **60**, 034017 (1999).
[12] A. H. Hoang, Z. Ligeti, and A. V. Manohar, Phys. Rev. D **59**, 074017 (1999); Phys. Rev. Lett. **82**, 277 (1999).
[13] A. J. Buras and M. Munz, Phys. Rev. D **52**, 186 (1995); M. Misiak, Nucl. Phys. **B393**, 23 (1993); [**B439**, 461(E) (1995).
[14] K. S. M. Lee and I. W. Stewart, hep-ph/0511334.
[15] G. P. Korchemsky and G. Sterman, Phys. Lett. B **340**, 96 (1994).
[16] M. Neubert, Phys. Rev. D **49**, 3392 (1994); **49**, 4623 (1994); I. I. Y. Bigi *et al.*, Int. J. Mod. Phys. A **9**, 2467 (1994).
[17] F. J. Tackmann, Phys. Rev. D **72**, 034036 (2005).
[18] C. W. Bauer *et al.*, Phys. Rev. D **70**, 094017 (2004).
[19] C. W. Bauer, S. Fleming, and M. E. Luke, Phys. Rev. D **63**, 014006 (2001); C. W. Bauer *et al.*, Phys. Rev. D **63**, 114020 (2001).
[20] C. W. Bauer and I. W. Stewart, Phys. Lett. B **516**, 134 (2001); C. W. Bauer, D. Pirjol, and I. W. Stewart, Phys. Rev. D **65**, 054022 (2002).
[21] C. W. Bauer and A. V. Manohar, Phys. Rev. D **70**, 034024 (2004).
[22] S. W. Bosch *et al.*, Nucl. Phys. **B699**, 335 (2004).
[23] A. K. Leibovich, I. Low, and I. Z. Rothstein, Phys. Rev. D **62**, 014010 (2000).
[24] K. S. M. Lee *et al.*, to be published.